Available online at www.sciencedirect.com
SCIENCE DIRECT®
Journal of Luminescence 113 (2005) 121–128
JOURNAL OF LUMINESCENCE
www.elsevier.com/locate/jlumin

Optical absorption and photoluminescence in Sm^{3+}- and Eu^{3+}-doped rare-earth borate glasses

Hai Lin[a,*], Dianlai Yang[a], Guishan Liu[a], Tiecheng Ma[a], Bin Zhai[a], Qingda An[a], Jiayou Yu[a], Xiaojun Wang[b], Xingren Liu[b], Edwin Yue-Bun Pun[c]

[a]*Faculty of Chemical Engineering and Materials, Dalian Institute of Light Industry, Dalian 116034, PR China*
[b]*Changchun Institute of Optics, Fine Mechanics and Physics, Chinese Academy of Sciences, Changchun 130021, PR China*
[c]*Department of Electronic Engineering, City University of Hong Kong, Tat Chee Avenue, Kowloon, Hong Kong, PR China*

Available online 8 December 2004

Abstract

Sm^{3+}- and Eu^{3+}-doped rare-earth borate glasses (Li_2O–BaO–La_2O_3–B_2O_3) have been fabricated and characterized optically. The density, refractive index, optical absorption, Judd-Ofelt parameters, and spontaneous transition probabilities have been measured, calculated and analyzed. Sm^{3+} and Eu^{3+} emit intense reddish-orange and red lights under blue and UV light excitations, respectively. In Sm^{3+} and Eu^{3+} co-doped glasses, the excitation wavelength range of Eu^{3+} emission is broadened owing to the energy transfer from Sm^{3+} to Eu^{3+}. This broadening makes the Ar^+ 488 nm wavelength laser a powerful excitation source for Eu^{3+} fluorescence. The rare-earth doped glasses with various visible emissions are useful for developing new color light sources, fluorescent display devices, UV-sensor and tunable visible lasers.

PACS: 78.40.ha; 78.55.qr

Keywords: Rare-earth borate glass; Optical absorption; Photoluminescence

1. Introduction

Rare-earth ions doped glasses are important materials for bulk lasers, optical fibers, waveguide lasers and optical amplifiers [1–4]. Trivalent rare-earth ions Er^{3+}- and Tm^{3+}-doped phosphate, silicate, germanate and tellurite glasses have been developed for infrared active optical devices [5–9]. Recently, research focus on rare-earth doped glasses is not limited to infrared optical devices, and there is a growing interest in visible optical devices [10–14]. With the increasing demand of various visible lasers and light sources, further investigations in other

*Corresponding author. Tel.: +86 411 84415969; fax: +86 411 86322228
E-mail addresses: lhai@dlili.edu.cn, lhai8686@yahoo.com (H. Lin).

0022-2313/$ - see front matter © 2004 Elsevier B.V. All rights reserved.
doi:10.1016/j.jlumin.2004.09.115

rare-earth ions, such as Sm^{3+} and Eu^{3+} ions, are becoming more significant [15–20].

Oxide glasses are attracting hosts for obtaining efficient luminescence in rare-earth ions. In them, borate glass is a suitable optical material with high transparency, low melting point, high thermal stability, and good rare-earth ions solubility [19,20]. However, interest in borate glass is small due to its high phonon energy, and it is difficult to obtain high efficient infrared and upconversion visible emissions in Er^{3+}, Tm^{3+} and Ho^{3+}. On the other hand, the high phonon energy in borate glass is not detrimental to Sm^{3+} and Eu^{3+} normal $4f$ transition emissions, and sometimes it can accelerate the relaxation processes, which is necessary and beneficial for visible emissions. In this work, borate glass as a suitable host for Sm^{3+} and Eu^{3+} is demonstrated. Optical absorption, Judd–Ofelt parameters and spontaneous transition probabilities were recorded and calculated. Efficient reddish-orange light in Sm^{3+} and red light in Eu^{3+} were measured and characterized, respectively. In Sm^{3+} and Eu^{3+} co-doped glass system, the excitation wavelength range of Eu^{3+} emission is broadened owing to the energy transfer from Sm^{3+} to Eu^{3+}. These rare-earth doped borate glasses with various visible emissions will be useful in developing new light sources, display devices, UV-sensors and tunable visible lasers.

2. Experiments

The molar compositions of Sm^{3+} and Eu^{3+} doped Li_2O–BaO–La_2O_3–B_2O_3 (LBLB) glasses are $8Li_2O \cdot 7BaO \cdot (15-m-n)La_2O_3 \cdot 70B_2O_3$:$mSm_2O_3$, nEu_2O_3. The raw materials were Li_2CO_3, $BaCO_3$, La_2O_3, H_3BO_3, Sm_2O_3 and Eu_2O_3, and all the chemical powders were 99.5%–99.999% purity. The well-mixed materials were first heated for 30 min in an Al_2O_3 crucible at 800°C using an electric furnace, and then at a higher melting temperature of 1150°C for 2 h. The glasses were obtained by pouring the melt into a preheated brass mould. The samples were subsequently annealed at lower temperatures and then sliced and polished. For optical measurements, the annealed glass samples were sliced and polished to dimensions 20 mm × 20 mm × 3.1 mm. The density of these glass samples was measured to be 3.36g/cm^3, thus the number density of Sm^{3+} and Eu^{3+} ions can be calculated by

$$N = \frac{\rho}{M_{\text{total}}} \times M_c \times 2 \times A_v, \tag{1}$$

where N is the number density of rare-earth ions, ρ is the glass density, M_c is the molar percent concentration of rare-earth oxide, M_{total} is the sum of molecular weights in rare-earth borate glass ($8Li_2O \cdot 7BaO \cdot 14La_2O_3 \cdot 70B_2O_3$:$1Sm_2O_3$ or $8Li_2O \cdot 7BaO \cdot 14La_2O_3 \cdot 70B_2O_3$:$1Eu_2O_3$) and A_v is Avogadro's number. Both the number density of Sm^{3+} and Eu^{3+} ions in LBLB:$1.0Sm_2O_3$ and LBLB:$1.0Eu_2O_3$ glasses are estimated to be 3.65×10^{20}/cm^3.

The refractive indices (n) of the glass were measured using an Abbe refractometer at sodium wavelength and $n_{\text{meas}} = 1.6414$. Absorption spectra were recorded with a Perkin–Elmer Lamda 35 UV–VIS double-beam spectrometer. The excitation and fluorescence spectra of the samples were measured at room temperature using a Hitachi MPF-4 spectrophotometer and a 75-W xenon lamp source.

3. Results and discussion

Absorption spectra of LBLB:$1.0Sm_2O_3$ and LBLB:$1.0Eu_2O_3$ glasses are shown in Figs. 1 and 2, respectively. Assignments of the bands for the excited states from the ground states of Sm^{3+} and Eu^{3+} are also indicated in Figs. 1 and 2, respectively. The radiative transition within the $4f^n$ configuration of a rare-earth ion can be analyzed by the Judd–Ofelt approach [21,22]. According to the Judd–Ofelt theory, the oscillator strength, $P_{\text{calc}}[(S,L)J;(S',L')J']$, of an electric-dipole absorption transition from the initial state $|(S,L)J\rangle$, to the final state $|(S',L')J'\rangle$, depends on three Ω_t parameters ($t = 2,4,6$) as

$$P_{\text{calc}}[(S,L)J;(S',L')J'] = \frac{8\pi^2 mc}{3h\lambda(2J+1)} \frac{(n^2+2)^2}{9n} \times \sum_{t=2,4,6} \Omega_t \left|\langle (S,L)J \| U^{(t)} \| (S',L')J' \rangle\right|^2, \tag{2}$$

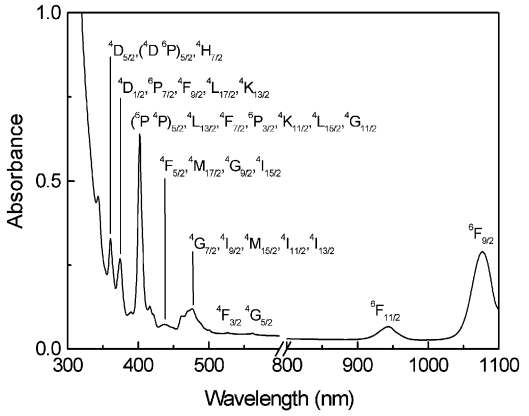

Fig. 1. Absorption spectrum of Sm^{3+}-doped Li_2O–BaO–La_2O_3–B_2O_3 glasses. (Number density of $Sm^{3+} = 3.65 \times 10^{20}$/cm^3).

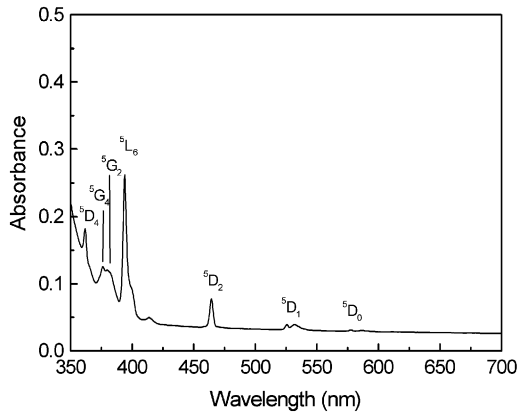

Fig. 2. Absorption spectrum of Eu^{3+}-doped Li_2O–BaO–La_2O_3–B_2O_3 glasses. (Number density of $Eu^{3+} = 3.65 \times 10^{20}$/cm^3).

where λ is the mean wavelength of the transition, m is the mass of the electron, c is the velocity, n is the refractive index, h is the Planck constant, Ω_t are the Judd–Ofelt parameters. The term $\left|\left\langle (S,L)J||U^{(t)}||(S',L')J'\right\rangle\right|^2$ is the square of the matrix elements of the tensorial operator, which connects $\left|(S,L)J\right\rangle$ to $\left|(S',L')J'\right\rangle$ states and is considered to be independent of host matrix.

The experimental oscillator strengths P_{exp} of the transitions can be obtained by integrating absorbance for each band and the relationship is

$$P_{\exp} = \frac{mc^2}{\pi e^2 N} \int \alpha(\bar{\nu})\, \mathrm{d}\bar{\nu}, \tag{3}$$

$$\alpha(\bar{\nu}) = \frac{\ln\left[I_0(\bar{\nu})/I(\bar{\nu})\right]}{d} = 2.303E(\bar{\nu})/d, \tag{4}$$

where N is the number density of rare-earth ions, e is the charge of the electron, $\bar{\nu}$ is the wavenumber, $E(\bar{\nu})$ is the absorbance, and d is the sample thickness.

The Judd–Ofelt intensity parameters Ω_t were derived from the electric-dipole contributions of the experimental oscillator strengths using a least-squares fitting approach. The squares of the matrix elements given in Ref. [23] were used in the calculation. The measured and calculated oscillator strengths, and Judd–Ofelt intensity parameters of Sm^{3+} and Eu^{3+} in LBLB glasses are presented in Tables 1 and 2, respectively. The measures of the fitting is given by the root-mean-square deviation δ_{rms} between the measured and the calculated oscillator strengths, and the relationship is

$$\delta_{\mathrm{rms}} = \left[\text{sum of squares deviations} / (\text{number of transitions} - \text{number of parameters})\right]^{1/2}. \tag{5}$$

Ω_t are important for investigating structure and transition properties of rare-earth ions. The calculated values of Ω_2, Ω_4, Ω_6 for Sm^{3+}- and Eu^{3+}-doped LBLB glasses are 6.81×10^{-20}, 4.43×10^{-20}, 2.58×10^{-20} and 8.78×10^{-20}, 6.12×10^{-20}, 1.94×10^{-20}, respectively. Here, Ω_2 in Eu^{3+} doped LBLB glasses is much higher than the values in zirconium fluoride and phosphate glasses, producing "hypersensitive pseudoquadrupolar transitions" having intensities (proportional to the genuine electric quadrupolar transitions, but with a huge factor) dependent almost exclusively on the square of $U^{(2)}$ [24]. In Sm^{3+} doped glasses, parameter Ω_2 is associated with the symmetry of the ligand field in the Sm^{3+} site [25]. The value of Ω_2 in LBLB glasses is larger than those in fluorozincate glasses [18], oxyfluoroborate glasses [26], zinc borosulphate glasses [27], lead fluoroborate glasses [25] and lead borate glasses [28], and is close to those in germanate glasses [29] and cadmium silicate glasses [17]. These behaviors suggest that the symmetry of the site occupied by Sm^{3+} in LBLB glasses is lower than those in the

Table 1
Experimental and calculated oscillator strengths of Sm^{3+} in Li_2O–BaO–La_2O_3–B_2O_3 glasses

Absorption from $^6H_{5/2}$	Energy (cm^{-1})	$P_{exp}(10^{-8})$	$P_{calc}(10^{-8})$
$^6F_{11/2}$	10588	121.3	148.7
$^6G_{5/2}$	17778	149.3	150.6
$^4F_{3/2}$	19011	648.5	643.6
$^4G_{7/2}$, $^4I_{9/2}$, $^4M_{15/2}$, $^4I_{11/2}$, $^4I_{13/2}$	21008	14.8	18.6
$^4F_{5/2}$, $^4M_{17/2}$, $^4G_{9/2}$, $^4I_{15/2}$	22883	134.9	123.2
$(^6P\ ^4P)_{5/2}$, $^4L_{13/2}$, $^4F_{7/2}$, $^6P_{3/2}$, $^4K_{11/2}$, $^4L_{15/2}$, $^4G_{11/2}$	24876	1.0	1.0
$^4D_{1/2}$, $^6P_{7/2}$, $^4F_{9/2}$, $^4L_{17/2}$, $^4K_{13/2}$	26738	1.1	2.1
$^4D_{3/2}$, $(^4D\ ^6P)_{5/2}$, $^4H_{7/2}$	27739	31.0	38.8
δ_{rms}		14.2×10^{-8}	
Ω_2 (cm^2)		6.81×10^{-20}	
Ω_4 (cm^2)		4.43×10^{-20}	
Ω_6 (cm^2)		2.58×10^{-20}	

Table 2
Experimental and calculated oscillator strengths of Eu^{3+} in Li_2O–BaO–La_2O_3–B_2O_3 glasses

Absorption from $^7F_0$	Energy (cm^{-1})	$P_{exp}(10^{-8})$	$P_{calc}(10^{-8})$
$^5D_2$	21529	17.4	30.1
$^5L_6$	25381	58.4	40.7
$^5G_2$, $^5G_4$	26316	123.8	123.3
$^5D_4$	27624	12.9	24.5
δ_{rms}		24.7×10^{-8}	
Ω_2 (cm^2)		8.78×10^{-20}	
Ω_4 (cm^2)		6.12×10^{-20}	
Ω_6 (cm^2)		1.94×10^{-20}	

glasses above, indicating higher mixing of the opposite parity electronic configurations, which are responsible for the spectral intensities. In addition, Ω_4/Ω_6 has been reported that it is the spectroscopic quality factor to characterize the glasses concerned [30]. In Sm^{3+}-doped LBLB glasses, the value is 1.72. It is larger than the values in zinc borosulphate, lead fluoroborate, lead borate, germanate and cadmium silicate glasses, and is similar to those in fluorzincate and oxyfluoroborate glasses, showing the Sm^{3+} -doped LBLB glass is a kind of better optical glasses.

Some important radiative properties can be calculated by use of the values of Ω_t[27,31]. The spontaneous transition probability is given by

$$A[(S,L)J;(S',L')J'] = A_{ed} + A_{md} = \frac{64\pi^4}{3h\lambda^3(2J+1)} \times \left[\frac{n(n^2+2)^2}{9}S_{ed} + n^3 S_{md}\right], \quad (6)$$

where A_{ed} and A_{md} are the electric-dipole and magnetic-dipole contribution, respectively. The electric-dipole and magnetic-dipole line strengths, S_{ed} and S_{md}, are expressed as

$$S_{ed} = e^2 \sum_{t=2,4,6} \Omega_t \left|\left\langle (S,L)J \middle\| U^{(t)} \middle\| (S',L')J' \right\rangle\right|^2, \quad (7)$$

$$S_{md} = \frac{e^2\hbar^2}{4m^2c^2}\left|\left\langle (S,L)J \middle\| L+2S \middle\| (S',L')J' \right\rangle\right|^2, \quad (8)$$

In this paper, the magnetic-dipole contribution is only considered for the $^5D_0 \rightarrow {}^7F_1$ magnetic-dipole transition of Eu^{3+}. The value of A_{md} was calculated using the value for $Ca_2Al_2SiO_7$ (A'_{md}) and corrected for the refractive index difference [31]. The relationship is

$$A_{md} = \left(\frac{n}{n'}\right)^3 A'_{md}, \quad (9)$$

where n (=1.64) and n' (=1.67) are the refractive indices of LBLB glass and $Ca_2Al_2SiO_7$, respectively.

The fluorescence branching ratio of transitions from initial manifold $|(S,L)J\rangle$ to lower levels $|(S',L')J'\rangle$ is given by

$$\beta[(S,L)J;(S',L')J'] = \frac{A[(S,L)J;(S',L')J']}{\sum_{S',L',J'} A[(S,L)J;(S',L')J']}. \quad (10)$$

The radiative lifetime of an emitting state is related to the total spontaneous emission probability for all transitions from this state by

$$\tau_{rad} = \left\{ \sum_{S',L',J'} A[(S,L)J;(S',L')J'] \right\}^{-1}. \quad (11)$$

Table 3 and 4 show the spontaneous transition probabilities, the branching ratios, and the calculated lifetimes of the optical transitions in Sm^{3+}- and Eu^{3+}-doped LBLB glasses. The predicated spontaneous-radiative transition rates for $^4G_{5/2} \rightarrow {}^6H_{9/2}$ and $^4G_{5/2} \rightarrow {}^6H_{7/2}$ transitions of Sm^{3+} are 200 and 139 s^{-1}, and the fluorescence branching ratios are 45% and 31%, respectively. The values are much higher than other emission transitions, indicating that the two transitions will be corresponding to main Sm^{3+} emission peaks. For Eu^{3+}, The predicated spontaneous-radiative transition rate for $^5D_0 \rightarrow {}^7F_2$ transition is 351 s^{-1}, and the fluorescence branching ratio is 64%, showing this transition can be expected to be the most intense emission in Eu^{3+}-doped LBLB glasses.

Sm^{3+} and Eu^{3+} single doped LBLB glasses emit bright reddish-orange and red lights under blue and UV light excitations, respectively. The emission spectra of Sm^{3+} and Eu^{3+} in LBLB glasses are shown in Fig. 3. The reddish-orange light from Sm^{3+} (curve 1) is composed of 563, 600 and 646 nm emission bands, corresponding to the $^4G_{5/2} \rightarrow {}^6H_J$ ($J = 5/2$, 7/2 and 9/2) transitions, respectively. The 600 nm emission band is the most intense and its full-width at half-maximum (FWHM) is 17 nm. The emission spectrum of Eu^{3+} in LBLB glasses (curve 2) consists of three

Table 3
Predicted spontaneous-radiative transition rates, fluorescence branching ratios and lifetimes of Sm^{3+} in Li_2O–BaO–La_2O_3–B_2O_3 glasses

Transition	Energy (cm^{-1})	$U^{(2)2}$	$U^{(4)2}$	$U^{(6)2}$	A_{ed} (s^{-1})	β(%)	τ_{rad} (ms)
$^4G_{5/2} \rightarrow {}^6F_{11/2}$	6851	0	0.0001	0.0005	0.27	0.06	2.25
$\rightarrow {}^6F_{9/2}$	8350	0.0018	0.0003	0.0002	3.97	0.89	
$\rightarrow {}^6F_{7/2}$	9637	0	0.0017	0.0002	3.49	0.79	
$\rightarrow {}^6F_{5/2}$	10493	0.0072	0.0017	0.0002	31.95	7.18	
$\rightarrow {}^6F_{3/2}$	11016	0.0011	0.0001	0	5.13	1.15	
$\rightarrow {}^6H_{15/2}$	11091	0	0	0.0002	0.34	0.08	
$\rightarrow {}^6F_{1/2}$	11203	0.0010	0	0	4.63	1.04	
$\rightarrow {}^6H_{13/2}$	12578	0	0.0002	0.0018	5.34	1.20	
$\rightarrow {}^6H_{11/2}$	14025	0	0.0053	0.0021	38.67	8.69	
$\rightarrow {}^6H_{9/2}$	15480	0.0112	0.0067	0.0020	199.74	44.89	
$\rightarrow {}^6H_{7/2}$	16667	0.0001	0.0086	0.0089	138.64	31.16	
$\rightarrow {}^6H_{5/2}$	17762	0.0003	0.0006	0	12.77	2.87	

Table 4
Predicted spontaneous-radiative transition rates, fluorescence branching ratios and lifetimes of Eu^{3+} in Li_2O–BaO–La_2O_3–B_2O_3 glasses

Transition	Energy (cm^{-1})	$U^{(2)2}$	$U^{(4)2}$	$U^{(6)2}$	A_{ed} (s^{-1})	A_{md} (s^{-1})	β(%)	τ_{rad} (ms)
$^5D_0 \rightarrow {}^7F_4$	14245	0	0.0023	0	118.3		22.11	1.87
$\rightarrow {}^7F_2$	16260	0.0032	0	0	351.3		65.65	
$\rightarrow {}^7F_1$	16920	0	0	0		65.5	12.24	

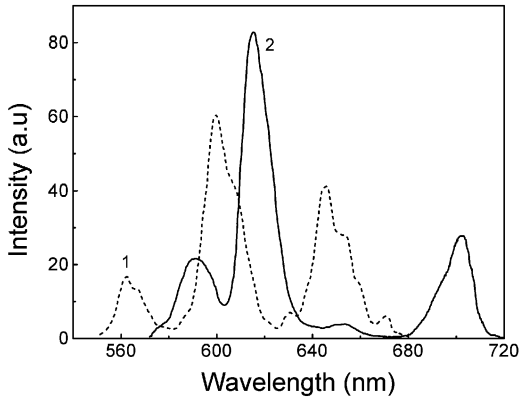

Fig. 3. Emission spectra of Sm^{3+} under 410 nm excitation (curve 1) and of Eu^{3+} under 397 nm excitation (curve 2).

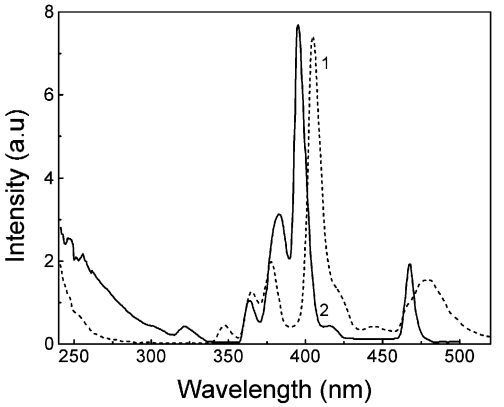

Fig. 4. Excitation spectra for 650 nm emission of Sm^{3+} (curve 1) and 597 nm emission of Eu^{3+} (curve 2).

intense emission bands peaking at 591, 615 and 702 nm and owing to the $^5D_0 \rightarrow {}^7F_J$ ($J = 1, 2, 4$) transitions, respectively. The main emission is the 615 nm red band and its FWHM is 15 nm.

The excitation spectra for 650 nm emission of Sm^{3+} and 597 nm emission of Eu^{3+} in LBLB glasses are given in Fig. 4. The excitation spectrum of Sm^{3+} (curve 1) is composed of eight bands peaking at ~240, 348, 365, 378, 405, 421, 445 and 479 nm, respectively. The broadband at ~240 nm is due to charge transfer state (CTS) of Sm^{3+}, and other sharp peaks are due to the $4f$–$4f$ inner shell transitions of Sm^{3+}. The excitation spectrum of Eu^{3+} (curve 2) consists of eight bands peaking at ~240, 321, 364, 383 395, 416, 421 and 468 nm, respectively. The broadband at ~240 nm and other seven peaks are due to the CTS and the $4f$–$4f$ transitions of Eu^{3+}.

In addition to single doped glass system, Sm^{3+} and Eu^{3+} co-doped LBLB glass (LBLB:0.1Sm_2O_3, 1.0Eu_2O_3) has been prepared. Emission bands due to efficient energy transfer from Sm^{3+} to Eu^{3+} were observed. The energy transfer occurs when 482 nm blue light was used as an excitation source. Under this excitation condition, there is no emission in Eu^{3+} single-doped LBLB glass because 482 nm wavelength is outside the absorption and excitation ranges of Eu^{3+} as shown above. However, in Sm^{3+} and Eu^{3+} co-doped system, 565, 600 and 646 nm emissions from Sm^{3+} plus 615 and 702 nm emissions from Eu^{3+} are observed, as shown in Fig. 5. The Eu^{3+} emission bands appearing in the Sm^{3+} emission spectrum indicates that a part of the absorption energy of Sm^{3+} has been transferred to Eu^{3+}. In particular, the most intensive emission in the spectrum is the 615 nm red peak of Eu^{3+}, and it confirms that the energy transfer from Sm^{3+} to Eu^{3+} is efficient. The existence of energy transfer expands the selectable pump source wavelength range for Eu^{3+} fluorescence. Hence, the 488 nm wavelength from argon laser is a powerful excitation source for Eu^{3+} red emission in Sm^{3+} and Eu^{3+} co-doped LBLB glass systems.

Comparison of Judd–Ofelt intensity parameters above shows that the absorption and emission transitions of Sm^{3+} and Eu^{3+} in LBLB glasses are more efficient than those in other glass hosts. It is beneficial to obtaining the powerful energy supply and transfer in co-doped glass system. The energy transfer process from Sm^{3+} to Eu^{3+} is shown in Fig. 6. When the $^4I_{9/2}$ level of Sm^{3+} is excited with 482 nm blue light, the initial population relaxes finally to the $^4G_{5/2}$ level. Part of the energy in the $^4G_{5/2}$ level of Sm^{3+} is transferred to the $^5D_0$ level of Eu^{3+} by resonance between the two energy levels. The energy transfer from Sm^{3+} to Eu^{3+} is almost irreversible, because the $^4G_{5/2}$ level in Sm^{3+} is about 600 cm^{-1} higher than the $^5D_0$ level in Eu^{3+}, and the probability in emitting phonons for

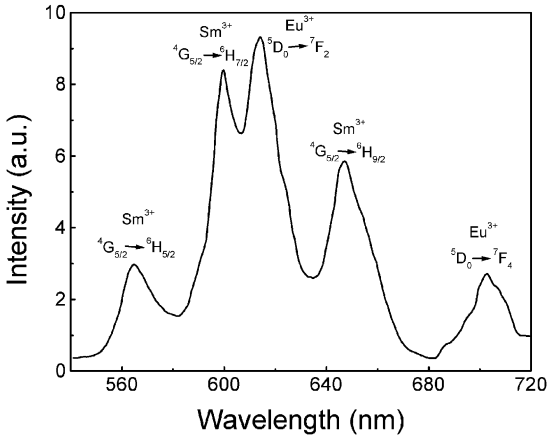

Fig. 5. Emission spectrum of Sm^{3+}- and Eu^{3+}-co-doped LBLB glasses under 482 nm excitation.

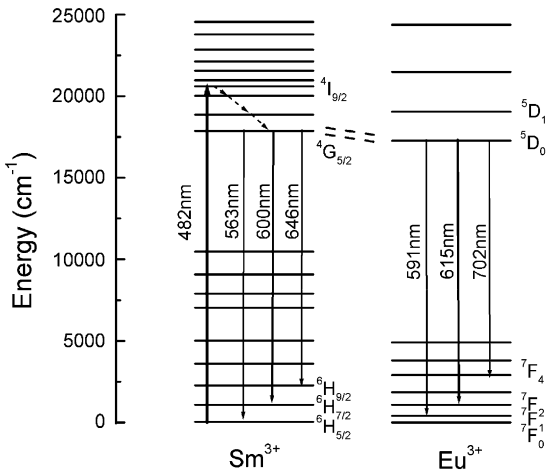

Fig. 6. Energy level diagrams and visible emission transitions of Sm^{3+} and Eu^{3+}. Energy transfer process from Sm^{3+} to Eu^{3+} is indicated.

Sm^{3+} $^4G_{5/2}$ → Eu^{3+} $^5D_0$ process is much higher than that in capturing phonons for Eu^{3+} $^5D_0$ → Sm^{3+} $^4G_{5/2}$ process. The energy resonance transfer enhances the population of Eu^{3+} $^5D_0$ level. The increment of the population due to the co-doping with Sm^{3+} causes the sensitization of Eu^{3+} emission under certain excitation conditions, and leads to the expansion of excitation range in Eu^{3+} fluorescence.

4. Conclusions

Sm^{3+}- and Eu^{3+}-doped rare-earth borate glasses have been synthesized and characterized. Judd–Ofelt intensity parameters Ω_2, Ω_4, Ω_6 for Sm^{3+} and Eu^{3+} doped LBLB glasses were derived from absorption spectra and the values are 6.81×10^{-20}, 4.43×10^{-20}, 2.58×10^{-20} and 8.78×10^{-20}, 6.12×10^{-20}, 1.94×10^{-20}, respectively. Intense reddish-orange and red lights are observed in Sm^{3+} and Eu^{3+} single-doped glasses, respectively, under blue and UV light excitations. In Sm^{3+} and Eu^{3+} co-doped system, the excitation wavelength range for Eu^{3+} emission is broadened due to the energy transfer from Sm^{3+} to Eu^{3+}. The broadening makes the 488 nm wavelength Ar^+ laser a powerful source for Eu^{3+} fluorescence. These glasses can be excited efficiently using commercial UV and blue laser diodes and LEDs, and can be used for developing new color light sources, fluorescent display devices, UV-sensors and tunable visible lasers.

Reference

[1] N. Chiodini, A. Paleari, G. Brambilla, E.R. Taylor, Appl. Phys. Lett. 80 (2002) 4449.
[2] P.R. Biju, G. Jose, V. Thomas, V.P.N. Nampoori, N.V. Unnikrishnan, Opt. Mat. 24 (2004) 671.
[3] S.D. Jackson, Appl. Phys. Lett. 83 (2003) 1316.
[4] B.N. Samson, J.A. Medeiros Neto, R.I. Laming, D.W. Hewak, Electron. Lett. 30 (1994) 1617.
[5] A. Mori, K. Kobayashi, M. Yamada, T. Kanamori, K. Oikawa, Y. Nishida, Y. Ohishi, Electron. Lett. 34 (1998) 887.
[6] H. Lin, E.Y.B. Pun, S.Q. Man, X.R. Liu, J. Opt. Soc. Am. B 18 (2001) 602.
[7] G. Jose, G. Sorbello, S. Taccheo, E. Cianci, V. Foglietti, P. Laporta, J. Non-Crystal. Solids 322 (2003) 256.
[8] N.O. Dantas, F. Qu, J.T. Arantes Jr., J. Alloy. Comp. 344 (2002) 316.
[9] S. Tanabe, X. Feng, T. Hanada, Opt. Lett. 25 (2000) 817.
[10] J. Hao, J. Gao, M. Cocivera, Appl. Phys. Lett. 82 (2003) 2224.
[11] S. Schweizer, L.W. Hobbs, M. Secu, J. Spaeth, A. Edgar, G.V.M. Williams, Appl. Phys. Lett. 83 (2003) 449.
[12] P.E.A. Mobert, E. Heumann, G. Huber, B.H.T. Chai, Appl. Phys. Lett. 73 (1998) 139.
[13] D.A. Turnbull, S.Q. Gu, S.G. Bishop, J. Appl. Phys. 80 (1996) 2436.
[14] T. Tsuboi, Eur. Phys. J. Appl. Phys. 26 (2004) 95.
[15] D. Ruter, W. Bauhofer, Appl. Phys. Lett. 69 (1996) 892.

[16] M.C. Farries, P.R. Morkel, J.E. Townsend, IEE Proc. 137 (1990) 318.
[17] H. Lin, E.Y.B. Pun, L.H. Huang, X.R. Liu, Appl. Phys. Lett. 80 (2002) 2642.
[18] V.D. Rodriguez, I.R. Martin, R. Alcala, R. Cases, J. Lumin 54 (1992) 231.
[19] N. Soga, K. Hirao, M. Yoshimoto, H. Yamamoto, J. Appl. Phys. 63 (1988) 4451.
[20] S.M. Kaczmarek, Opt. Mat. 19 (2002) 189.
[21] B.R. Judd, Phys. Rev. 127 (1962) 750.
[22] G.S. Ofelt, J. Chem. Phys. 37 (1962) 511.
[23] W.T. Carnall, P.R. Fields, K. Rajnak, J. Chem. Phys. 49 (1968) 4424.
[24] B. Blanzat, L. Boehm, C.K. Jorgensen, R. Reisfeld, N. Spector, J. Solid State Chem. 32 (1980) 185.
[25] A.G. Souza Filho, J. Mendes Filho, F.E.A. Melo, M.C.C. Custodio, R. Lebullenger, A.C. Hernandes, J. Phys. Chem. Solids 61 (2000) 1535.
[26] K.K. Mahato, D.K. Rai, S.B. Rai, Solid State Comm. 108 (1998) 671.
[27] C.K. Jayasankar, E. Rukmini, Opt. Mat. 8 (1997) 193.
[28] M.B. Saisudha, J. Bamakrishna, Phys. Rev. B 53 (1996) 6186.
[29] L. Boehm, R. Reisfeld, N. Spector, J. Solid State Chem. 28 (1979) 75.
[30] R.R. Reddy, Y.N. Ahammed, P.A. Azeem, K.R. Gopal, T.V.R. Rao, S. Buddhudu, N.S. Hussain, J. Quant. Spectrosc. Radiative Transfer 77 (2003) 149.
[31] X.H. Chai, H.J. Zhang, F.Sh. Li, K.Ch. Chou, Opt. Mat. 25 (2004) 301.